Optimization of silver nanoparticle biosynthesis by estuarine-derived Lactobacillus apis and characterization of capping biomolecules

Aravindan Baskaran[1], **Sivasubramani Kandasamy**[1*], **Dharmadevi Devaraj**[1], **Gayathri Sivakumar**[1], **Akshaya Dhanapal**[1], **Sekar Harikrishnan**[1]

[1]Email: aravindan386@gmail.com

[1*]Email: sivasubramanik@gmail.com

[1]Email: princydharma75@gmail.com

[1]Email: gayu2304@gmail.com

[1]Email: akshaya.dd18502gmail.com

***Corresponding Author:** Sivasubramani Kandasamy | Email: sivasubramanik@gmail.com

Abstract

The biological synthesis of silver nanoparticles (AgNPs) using microorganisms is a sustainable alternative to conventional physicochemical methods. An estuarine bacterial isolate exhibiting extracellular AgNP biosynthesis was recovered from sediment samples from the Arasalar Estuary, India, and identified as *Lactobacillus apis* SNSEB 3 based on 16S rRNA gene sequence analysis. Extracellular AgNP production was optimized by varying nutritional and environmental parameters. Starch and peptone were the most suitable carbon and nitrogen sources, while a carbon-to-nitrogen ratio of 1:1, agitation at 200 rpm, and a reaction time of 18 h resulted in maximal nanoparticle production. Optimization improved nanoparticle quality, reducing average particle diameter from 112.3 ± 3.9 nm to 20.9 ± 0.3 nm and the polydispersity index from 0.22 ± 0.01 to 0.03 ± 0.00. UV–visible spectroscopy revealed a surface plasmon resonance peak at 353.01 nm. Dynamic light scattering and transmission electron microscopy confirmed predominantly spherical nanoparticles with an average size of approximately 20 nm. X-ray diffraction showed the crystalline nature of the AgNPs, and energy-dispersive X-ray spectroscopy confirmed elemental silver. Biochemical characterization of the nanoparticle-associated capping matrix revealed fatty acids (46.2 ± 2.2%), proteins (30.1 ± 1.1%), and carbohydrates (23.7 ± 0.9%). Fourier-transform infrared spectroscopy identified hydroxyl, amide, peptide, ester, alkane, and glycosidic functional groups, indicating biomolecules in nanoparticle stabilization.

Keywords

Lactobacillus apis, silver nanoparticles, Nanoparticle stabilization, Capping biomolecules.

How to cite this article: Baskaran A, Kandasamy S, Devaraj D, Sivakumar G, Dhanapal A, Harikrishnan S. Optimization of silver nanoparticle biosynthesis by estuarine-derived Lactobacillus apis and characterization of capping biomolecules. Int J Drug Deliv Technol. 2026;16(79s): 139-146. DOI: 10.25258/ijddt.16.79s.15

Introduction

Silver nanoparticles (AgNPs) have emerged as a central focus in nanomaterial research, attributed to their unique physicochemical properties and broad-spectrum antimicrobial efficacy. Their high surface-area-to-volume ratio, catalytic activity, and ability to interact with microbial membranes and intracellular targets have enabled their application across various fields, including medicine, food preservation, environmental remediation, and biotechnology[1]. Conventional nanoparticle synthesis methods primarily employ chemical reducing agents and physical processes, which often require substantial energy inputs and may generate hazardous by-products. Consequently, there is an increasing emphasis on developing environmentally sustainable nanoparticle production techniques.[2,3]

The biological synthesis of nanoparticles using microorganisms has attracted considerable interest as an eco-friendly alternative to physicochemical methods. In microbial systems, extracellular metabolites, enzymes, proteins, polysaccharides, and other biomolecules can function as both reducing and stabilizing agents, thereby eliminating the need for toxic chemicals[4]. Biologically synthesized nanoparticles often exhibit enhanced biocompatibility and stability due to naturally occurring capping molecules on the nanoparticle surface. Recent studies have successfully demonstrated the synthesis of AgNPs using bacteria, fungi, algae, and plant-derived biomaterials, highlighting the versatility of biological nano factories[5,6]. Within bacterial systems, Lactic Acid Bacteria (LAB) are particularly promising for green nanoparticle synthesis. LAB are generally recognized as safe (GRAS) and produce a variety of extracellular metabolites, exopolysaccharides, and proteinaceous compounds that facilitate metal ion reduction and nanoparticle stabilization[7,8]

Several *Lactobacillus* species have been reported to synthesize AgNPs with notable

antimicrobial properties. For example, AgNPs synthesized using *Lactobacillus plantarum* and *Lactobacillus brevis* exhibited spherical morphology with particle sizes ranging from 5 to 40 nm and demonstrated significant antibacterial activity against both Gram-positive and Gram-negative pathogens[9]. Similarly, different *Lactobacillus* strains produced AgNPs with varying particle sizes and antibacterial activities, indicating that strain-specific extracellular or capsular biopolymers influence nanoparticle formation and stabilization[10]. Moreover, AgNPs synthesized using *Lactobacillus bulgaricus* exhibited substantial antibacterial activity against clinically relevant bacterial pathogens, underscoring the potential of LAB as sustainable nanobiotechnological platforms[11].

The physicochemical properties of AgNPs, including particle size, dispersity, morphology, crystallinity, and surface chemistry, are significantly influenced by cultivation conditions and synthesis parameters. Optimization of nutritional and environmental factors such as carbon and nitrogen sources, carbon-to-nitrogen ratio, agitation, and reaction time can markedly affect nanoparticle yield and quality[12,13]. Smaller and more monodisperse nanoparticles generally exhibit enhanced biological activity due to their increased surface reactivity and greater interaction with microbial cells. Therefore, systematic optimization of biosynthetic conditions is crucial for developing reproducible and scalable microbial nanoparticle production processes [14,15].

While the biosynthesis of nanoparticles by terrestrial and food-associated Lactobacillus species has been extensively documented, research on the nanoparticle-producing capabilities of lactic acid bacteria derived from estuarine environments remains limited. [16,17]. Existing studies primarily focus on nanoparticle production and their antimicrobial properties, with insufficient attention given to the biochemical composition of the capping matrices associated with nanoparticles and their role in stabilization[18]. To the best of our knowledge, no studies have reported the optimization of extracellular silver nanoparticle biosynthesis by estuarine *L. apis* or the comprehensive characterization of nanoparticle-associated capping biomolecules involved in nanoparticle stabilization.

Materials and Methods

Bacterial strain and culture conditions

Sediment samples were collected from the Arasalar Estuary (Latitude 10º91’32.15”N, Longitude 79º84’94.45”E), located in Karaikal, Puducherry, India, in May 2025. The samples were collected using sterile equipment and transported to the laboratory under refrigerated conditions (4°C). Through serial dilution and spread plating on nutrient agar, which was prepared with synthetic estuarine water (25 ppt salinity, pH 7.8 ± 0.2), eleven morphologically distinct bacterial isolates were recovered. These isolates were screened for their ability to biosynthesize extracellular silver nanoparticles (AgNPs) using cell-free culture supernatants and UV–visible spectroscopic analysis. Among the isolates SNSEB 3 demonstrated the highest potential for AgNP synthesis and was selected for further study.

The molecular identification of SNSEB 3 was conducted by partially sequencing the 16S rRNA gene using universal primers 27F and 1492R [19]. Sequence similarity analysis was performed using the NCBI BLAST database, and phylogenetic relationships were inferred through the Neighbor-Joining, MEGA11 [20]. The isolate was identified as *Lactobacillus apis*, and the 16S rRNA gene sequence was deposited in the NCBI GenBank database under accession number PV927163.1. The strain was maintained on nutrient agar prepared with synthetic estuarine water (25 ppt salinity, pH 7.8 ± 0.2) and stored at 4°C. Unless specified otherwise, cultures were grown in nutrient broth prepared with estuarine water at 37°C.

Growth kinetics and optimization of AgNP biosynthesis

For the biosynthesis of AgNPs, *L. apis* SNSEB 3 was cultured in 100 mL Erlenmeyer flasks containing 40 mL of broth medium. The inoculum was derived from exponentially growing cultures and adjusted to an OD_{620} of 0.1, equating to approximately $1 \times 10^{\wedge 8}$ CFU mL^{-1}. The basal fermentation conditions were maintained at pH 7.8 ± 0.2, 37°C, with 150 rpm agitation, 1% fructose, 0.5% yeast extract, and 25 ppt salinity.

Growth kinetics and nanoparticle production were assessed at 12-hour intervals up to 144 hours. Cell biomass was collected by centrifugation at 3000 × g for 15 minutes, dried at 50°C, and quantified as dry weight (g/L^{-1}). Cell-free supernatants were utilized for AgNP biosynthesis and spectroscopic analysis.

To optimize AgNP production, fermentation parameters were individually varied using a one-factor-at-a-time methodology. Carbon sources, including glucose, fructose, lactose, maltose, cellulose, and starch, were evaluated at 1% (w/v), while nitrogen sources such as peptone, yeast extract, malt extract, beef extract, ammonium nitrate, and ammonium sulphate were tested at 0.5% (w/v). Carbon-to-nitrogen ratios of 0.25:1, 0.5:1, 1:1, 1:0.5, and 1:0.25 were subsequently investigated. Agitation rates from 0 to 300 rpm and nanoparticle reaction times between 6 and 30 hours were also examined.

For nanoparticle synthesis, equal volumes of cell-free supernatant and 0.01 M AgNO3 solution were combined and incubated at room temperature (28°C). The formation of AgNPs was

indicated by the development of a yellow-brown colour and confirmed through UV–Vis spectroscopy[21–23].

Effect of optimization on nanoparticle size and dispersity

Nanoparticles synthesized under each optimized condition were subjected to analysis using a nanoparticle size analyser (NANOPLUS, Particulate Systems, USA) employing dynamic light scattering (DLS)[24]. The hydrodynamic diameter and polydispersity index (PDI) were documented to evaluate particle size distribution and dispersity. Measurements were conducted in triplicate and reported as mean ± standard deviation.

Characterization of biosynthesized AgNPs

Silver nanoparticles (AgNPs) synthesized under optimized conditions were isolated through centrifugation at 10,000 rpm for 20 minutes. The resulting pellet underwent three washes with phosphate buffer (pH 7.0) and was subsequently dried at 50°C before characterization[21,22,24]. UV–Visible spectra were obtained using a UV-2600i spectrophotometer (Shimadzu, USA[25]. The particle size distribution was assessed via dynamic light scattering (DLS) as previously described. The crystalline structure of the AgNPs was analysed using X-ray diffraction (XRD) on a Rigaku MiniFlex benchtop diffractometer, covering a diffraction angle range of 20–80° [26]. Transmission electron microscopy (TEM; JEM-2100, JEOL, Japan) operating at 200 kV was employed to examine morphology and particle size. Image processing was conducted using ImageJ and Gwyddion software. The elemental composition was determined through energy-dispersive X-ray spectroscopy (EDS) integrated with the TEM system.

Characterization of the nanoparticle capping agent

The biochemical composition of the nanoparticle-associated capping material was assessed for its protein, carbohydrate, and fatty acid contents. The total protein content was quantified employing bovine serum albumin as the standard [27]. The total carbohydrate content was estimated via the phenol–sulphuric acid method [28], with glucose serving as the standard. Total free fatty acids were quantified through alkali titration and expressed as acid value [29]. Functional groups within the nanoparticle capping matrix were identified using Fourier-transform infrared spectroscopy (FTIR). Dried AgNP samples were combined with KBr and analyzed using an IR Affinity-1 FTIR spectrometer (Shimadzu, Japan). Spectra were recorded in the range of 400 to 4000 cm−1 at a resolution of 4 cm−1, with 10 scans accumulated [30].

Results

Isolation and screening of silver nanoparticle-synthesizing bacteria

Eleven morphologically distinct bacterial isolates were obtained from sediment samples collected at the Arasalar Estuary, Karaikal, India, in May 2025 (supporting information: Figure S1).

These isolates were evaluated for their capacity to synthesise silver nanoparticles (AgNPs) using cell-free supernatants, assessed through UV–visible (UV–Vis) spectroscopic analysis. Strain SNSEB 3 demonstrated the highest absorbance at 0.774 OD (Figure 1), with a characteristic surface plasmon resonance peak at 398.01 nm, followed by SNSEB 8 with an absorbance of 0.392 OD (supporting information: Table S2, Figure S3).

The other isolates exhibited significantly lower absorbance values, ranging from 0.107 to 0.181 OD. Due to its superior potential for AgNP synthesis, SNSEB 3 was further confirmed as a pure culture (Figure 1) and selected for additional investigation.

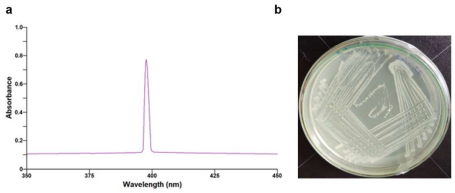

Figure 1. (a) Strain SNSEB 3 demonstrated the highest absorbance; (b) pure culture of *Lactobacillus apis*

Molecular identification of the selected isolate

The isolate SNSEB 3 was identified through partial sequencing of the 16S rRNA gene. BLAST analysis indicated a high sequence similarity to *Lactobacillus apis*. The sequence has been deposited in the NCBI GenBank database with the accession number PV927163.1. Phylogenetic analyses, conducted using the Neighbour-Joining method (Figure 2), corroborated the taxonomic identity of the isolate as *Lactobacillus apis*.

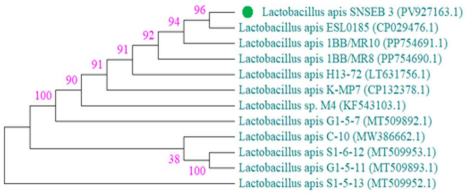

Figure 2. Phylogenetic tree of *Lactobacillus apis* SNSEB 3 with ITS regions

Growth kinetics and optimization of AgNP biosynthesis

The growth dynamics of *Lactobacillus apis* SNSEB 3 and the biosynthesis of AgNPs were observed over a period of 144 hours. The cell biomass exhibited a consistent increase from 0.98 g/L at 12 hours to a peak of 8.02 g/L at 84 hours,

after which a gradual decline was noted during the later incubation stages. AgNP production followed a similar pattern, with absorbance rising from 0.56 at 24 hours to a maximum of 7.76 at 96 hours. The corresponding wavelength shifted from 449.9 nm at 24 hours to 393.45 nm at 96 hours. Post 96 hours, both absorbance and biomass showed a progressive decrease (Fig. 3).

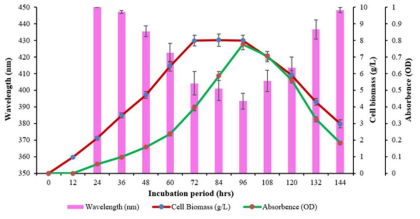

Figure 3: Growth dynamics of *Lactobacillus apis* SNSEB 3 and AgNPs biosynthesis

The impact of various carbon sources on AgNP biosynthesis was assessed using UV–Visible spectroscopy. Among the carbon sources tested, starch yielded the highest absorbance value of 0.859 at a wavelength of 388.71 nm, followed by cellulose (0.792) and fructose (0.777). Lower absorbance values were observed for glucose, maltose, and lactose (Fig. 4a). In terms of nitrogen sources, peptone resulted in the highest absorbance (0.895) at 379.39 nm, followed by yeast extract (0.859), whereas ammonium nitrate and ammonium sulphate produced relatively lower absorbance values (Fig. 4b). The study further explored the influence of carbon-to-nitrogen ratios. A 1:1 carbon-to-nitrogen ratio produced the highest absorbance value of 0.932 with a corresponding wavelength of 368.67 nm (Fig. 4c). Other ratios resulted in absorbance values ranging from 0.649 to 0.894. Agitation was found to affect AgNP biosynthesis significantly. Absorbance increased from 0.362 under static conditions to 0.961 at 200 rpm, with a concurrent reduction in wavelength from 447.8 to 357.72 nm (Fig. 4d).

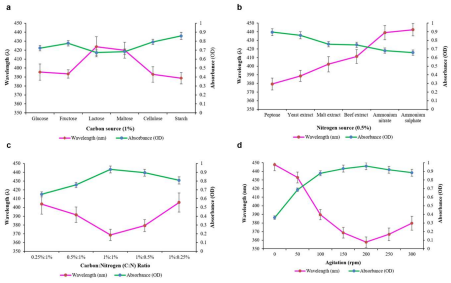

Figure 4: Impact of various energy sources on AgNP biosynthesis (a). Carbon Source (b). Nitrogen source (c). Carbon: Nitrogen ratio (1:1) (d). Agitation

Further increases in agitation speed led to a slight decrease in absorbance. Similarly, reaction time influenced nanoparticle formation, with absorbance rising from 0.562 at 6 hours to a peak of 0.998 at 18 hours, followed by a slight reduction at 24 and 30 hours (supporting information: Table S4).

Effect of optimization on nanoparticle size and dispersity

Dynamic light scattering (DLS) analysis was employed to assess the size distribution and dispersity of AgNPs synthesized under various optimization conditions. The AgNPs produced during the growth kinetics experiment demonstrated an average diameter of 112.3 ± 3.9 nm with a polydispersity index (PDI) of 0.22 ± 0.01.(Fig. 5a) Optimization using starch as a carbon source resulted in a reduction of particle size to 89.7 ± 3.1 nm and a PDI of 0.17 ± 0.01 (Fig. 5b). Further size reductions were achieved with the addition of peptone (63.2 ± 2.3 nm; PDI 0.11 ± 0.01) (Fig. 5c), 1:1 carbon-to-nitrogen ratio (49.7 ± 1.8 nm; PDI 0.07 ± 0.00) (Fig. 5d) and agitation at 200 rpm (34.8 ± 1.1 nm; PDI 0.05 ± 0.00) (Fig. 5e). The smallest particles, with an average diameter of 20.9 ± 0.3 nm and a PDI of 0.03 ± 0.00, were obtained after 18 hours of reaction (Fig. 5f).

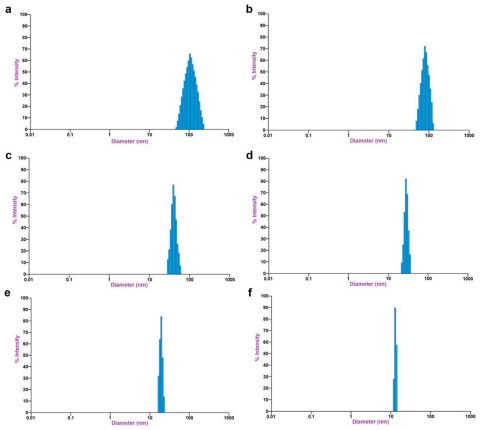

Figure 5. PDI analysis of AgNPs synthesised under various optimization conditions (a)96hr incubation (b) AgNPs at 1% starch (Carbon source) (c) AgNPs at 0.5% peptone (Nitrogen source) (d) AgNPs at 1:1 Carbon: Nitrogen ratio (e) AgNPs at 200 rpm agitation (f) AgNPs at 18hrs reaction time

Characterization of biosynthesized AgNPs

Silver nanoparticles (AgNPs) synthesized under optimized conditions were subjected to characterization through various analytical techniques, including UV–Visible spectroscopy, dynamic light scattering (DLS), X-ray diffraction (XRD), transmission electron microscopy (TEM) and energy-dispersive X-ray spectroscopy (EDS). UV–Visible spectroscopy identified a characteristic absorption peak at 353.01 nm with an absorbance of 0.999 (Fig. 6a). DLS analysis indicated an average particle size of 20.2 ± 0.3 nm and a polydispersity index (PDI) of 0.03 ± 0.00 (Fig. 6b).

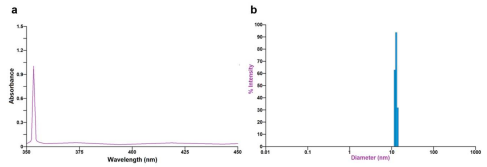

Figure 6: Characterisation of Silver nanoparticles (AgNPs) using UV–Visible spectroscopy and DLS method (a) characteristic absorption peak (b) DLS method showing 20.2±0.3nm size and 0.03±0.0 PDI

The crystalline structure of the AgNPs was verified through X-ray diffraction analysis, which revealed diffraction peaks at 2θ values of 38°, 44°, 64°, and 77°, corresponding to the (111), (200), (220), and (311) crystallographic planes, respectively (Fig. 7a). TEM analysis showed that the nanoparticles were predominantly spherical, with sizes ranging from 17.1 to 23.3 nm and an average diameter of 20.2 nm (Fig. 7b). EDS analysis detected a significant signal for silver at approximately 3 keV, along with signals for carbon, nitrogen, and oxygen (Fig. 7c).

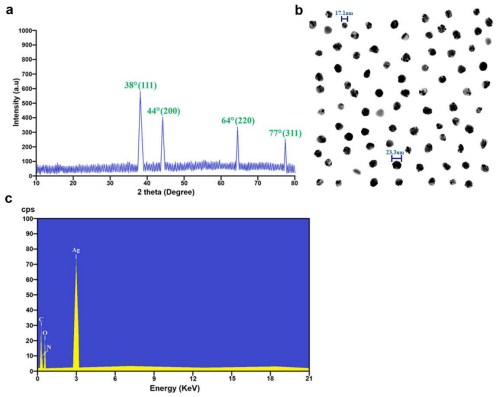

Figure 7: Characterisation of Silver nanoparticles using X-ray diffraction, TEM and EDS. (a) diffraction peaks (b) TEM analysis showing the size of the nanoparticles (c) EDS analysis showing significant signal for silver at approximately 3 keV, along with signals for carbon, nitrogen, and oxygen

Characterization of the nanoparticle capping agent

FTIR analysis of the capping material associated with nanoparticles revealed the presence of proteins (30.1 ± 1.1%), carbohydrates (23.7 ± 0.9%), and fatty acids (46.2 ± 2.2%). The spectrum showed absorption bands at 3229 cm^{-1}, which corresponds to hydroxyl groups; 3196 and 3106 cm^{-1}, which correspond to amide groups; 2954, 2925, 2871, 2854, 1403, and 1385 cm^{-1}, which correspond to alkane groups; 1654, 1631, and 1552 cm^{-1}, which correspond to peptide linkages; 1296 and 1237 cm^{-1}, which correspond to ester linkages; and 1136 cm^{-1}, which correspond to glycosidic linkages. Additional peaks were detected at 1462, 1057, and 1037 cm^{-1}, corresponding to carbon–carbon ring structures (Fig. 8).

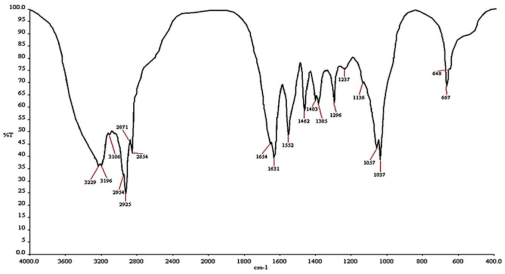

Figure 8: FTIR analysis of the capping material associated with nanoparticles

Discussion

The study demonstrates extracellular biosynthesis of silver nanoparticles (AgNPs) by an estuarine-derived strain of *L. apis*. The present study demonstrates the extracellular biosynthesis of silver nanoparticles (AgNPs) by an estuarine-derived strain of *Lactobacillus apis*. The synthesis of AgNPs using *Lactobacillus* species has been widely documented [31]; however, studies involving estuarine-derived lactic acid bacteria remain limited. The ability of *L. apis* SNSEB 3 to generate AgNPs extracellularly highlights estuarine environments as a source of nano-biotechnologically relevant microorganisms. AgNPs synthesized using cell free supernatant of SNSEB3 produced the highest surface plasmon resonance (SPR) peak, when compared to other isolates. This significant peak confirms the reduction of Ag^{+} ions to silver nanoparticles[32,33]. The shift in absorbance maxima during optimization suggests the production of smaller nanoparticles with improved physicochemical properties. Cell free supernatant is rich in metabolites whose composition and concentration varies during different stages of growth. These metabolites contribute to silver ion reduction aiding in synthesis of AgNPs. Similar observations in microbial nanoparticle synthesis systems show proteins, enzymes, polysaccharides, and other extracellular biomolecules function as reducing and stabilizing agents [4]. Biomass accumulation and nanoparticle production further support the role of metabolically active cultures in efficient AgNP biosynthesis.

Optimization experiments were conducted to identify the growth conditions and reaction parameters that promote efficient AgNP biosynthesis by *L. apis* SNSEB 3. Starch and peptone were suitable carbon and nitrogen sources, respectively, while a carbon-to-nitrogen ratio of 1:1, agitation at 200 rpm, and an 18 h reaction period yielded optimal nanoparticle formation. Previous studies have shown that nutrient composition and cultivation conditions influence nanoparticle biosynthesis by regulating microbial metabolism and secretion of reducing biomolecules [16,34].

The enhanced production of AgNPs under optimized conditions, comprising starch, peptone, a 1:1 carbon-to-nitrogen ratio, 200 rpm agitation, and an 18 h reaction time, may be attributed to the increased production of extracellular metabolites involved in silver ion reduction and nanoparticle stabilization. Optimization also reduced size and dispersity. The hydrodynamic diameter decreased from 112.3 nm to approximately 20 nm, with PDI reduced from 0.22 to 0.03, indicating a monodisperse nanoparticle population. Previous LAB-mediated AgNP synthesis studies reported particle sizes of approximately 5 to 40 nm, although uniformity varied among strains [32,33]. The monodisperse nanoparticles obtained suggest optimization improved yield and reproducibility. Smaller, more uniform nanoparticles are associated with increased surface reactivity and improved biological performance owing to their larger effective surface area [35]. Producing small, uniform silver nanoparticles (AgNPs) can improve colloidal stability, enhance reactivity, and increase their effectiveness in antimicrobial and biomedical applications. The findings underscore the importance of systematic optimization in creating reliable microbial platforms for synthesizing high-quality silver nanoparticles.

Characterization studies confirmed synthesis of crystalline spherical silver nanoparticles. The SPR peak observed by UV–Visible spectroscopy, together with the TEM-derived particle size range of 17–23 nm, agrees with reports on biologically synthesized AgNPs. The predominance of spherical nanoparticles is consistent with observations in *L. plantarum*, *L. bulgaricus*, and LAB-mediated synthesis systems [11,32] .

XRD peaks corresponding to the (111), (200), (220), and (311) planes confirmed the face-centered cubic structure of metallic silver, and EDS verified silver reduction and accumulation in the nanoparticle preparation. A key finding was characterization of the nanoparticle-associated capping matrix. Although most investigations focused on nanoparticle synthesis and antimicrobial activity, few quantitatively examined the biochemical composition of capping materials associated with AgNPs [5]. The matrix consisted predominantly of fatty acids, followed by proteins and carbohydrates. Because most reports on LAB-mediated nanoparticle synthesis emphasize proteins and exopolysaccharides as stabilizing biomolecules, this suggests fatty acids may play a larger role in nanoparticle stabilization than previously recognized. The FTIR spectra supported the involvement of multiple biomolecule classes in nanoparticle stabilization. Bands corresponding to hydroxyl, amide, alkane, ester, peptide, and glycosidic functional groups indicate proteins, carbohydrates, and lipid-derived compounds on the nanoparticle surface. Similar FTIR signatures have been reported for biologically synthesized AgNPs where extracellular biomolecules act as reducing and capping agents [5,36]. The coexistence of these groups suggests a complex biomolecular corona that contributes to stability and prevents aggregation.

Overall, the present study demonstrates that estuarine-derived *L. apis* effectively produces extracellular silver nanoparticles. Optimization processes enhanced the yield and resulted in the generation of monodisperse nanoparticles with an average size of approximately 20 nm. These findings significantly expand the current understanding of LAB-mediated nanoparticle synthesis.

Acknowledgement

Declarations

- The authors did not receive support from any organization for the submitted work.
- The authors have no conflicts of interest to declare that are relevant to the content of this article.
- The datasets generated during and/or analysed during the current study are available from the corresponding author on reasonable request.

Bibliography

[1] Almatroudi, A., 2020. Silver nanoparticles: synthesis, characterisation and biomedical applications. Open Life Sciences, 2020, 15, 819–839.

[2] Ahmed, S., Ahmad, M., Swami, B.L., Ikram, S., 2016. A review on plants extract mediated synthesis of silver nanoparticles for antimicrobial applications: A green expertise. Journal of Advanced Research, 2016, 7, 17–28.

[3] Halaris, A.E., Belendiuk, K.T., Freedman, D.X., 1975. Antidepressant drugs affect dopamine uptake. Biochem Pharmacol, 1975, 24, 1896–1897.

[4] Lahiri, D., Nag, M., Sheikh, H.I., Sarkar, T., et al., 2021. Microbiologically-Synthesized Nanoparticles and Their Role in Silencing the Biofilm Signaling Cascade. Front. Microbiol., 2021, 12, 636588.

[5] Sidhu, A.K., Verma, N., Kaushal, P., 2022. Role of Biogenic Capping Agents in the Synthesis of Metallic Nanoparticles and Evaluation of Their Therapeutic Potential. Front. Nanotechnol., 2022, 3, 801620.

[6] Witkowska, E., Godlewska, M., Osiejuk, J., Gątarz, S., et al., 2022. Bifunctional Opioid/Melanocortin Peptidomimetics for Use in Neuropathic Pain: Variation in the Type and Length of the Linker Connecting the Two Pharmacophores. IJMS, 2022, 23, 674.

[7] Velychko, T.P., Soldatkin, O.O., Melnyk, V.G., Marchenko, S.V., et al., 2016. A Novel Conductometric Urea Biosensor with Improved Analytical Characteristic Based on Recombinant Urease Adsorbed on Nanoparticle of Silicalite. Nanoscale Res Lett, 2016, 11, 106.

[8] Al-asbahi, M.G.S.S., Al-Ofiry, B.A., Saad, F.A.A., Alnehia, A., Al-Gunaid, M.Q.A., 2024. Silver nanoparticles biosynthesis using mixture of Lactobacillus sp. and Bacillus sp. growth and their antibacterial activity. Sci Rep, 2024, 14, 10224.

[9] Mohd Yusof, H., Abdul Rahman, N., Mohamad, R., Zaidan, U.H., 2020. Microbial Mediated Synthesis of Silver Nanoparticles by Lactobacillus Plantarum TA4 and its Antibacterial and Antioxidant Activity. Applied Sciences, 2020, 10, 6973.

[10] Velychko, T.P., Soldatkin, O.O., Melnyk, V.G., Marchenko, S.V., et al., 2016. A Novel Conductometric Urea Biosensor with Improved Analytical Characteristic Based on Recombinant Urease Adsorbed on Nanoparticle of Silicalite. Nanoscale Res Lett, 2016, 11, 106.

[11] Naseer, Q.A., Xue, X., Wang, X., Dang, S., et al., 2022. Synthesis of silver nanoparticles using Lactobacillus bulgaricus and assessment of their antibacterial potential. Braz. J. Biol., 2022, 82, e232434.

[12] An, Y., Zhang, L., Xiong, S., Wu, S., et al., 2012. Fluorine-containing thermo-sensitive microgels as carrier systems for biomacromolecules. Colloids and Surfaces B: Biointerfaces, 2012, 92, 246–253.

[13] Korbekandi, H., Iravani, S., Abbasi, S., 2012. Optimization of biological synthesis of silver nanoparticles using *Lactobacillus casei* subsp. *casei*. J of Chemical Tech & Biotech, 2012, 87, 932–937.

[14] Morones, J.R., Elechiguerra, J.L., Camacho, A., Holt, K., et al., 2005. The bactericidal effect of silver nanoparticles. Nanotechnology, 2005, 16, 2346–2353.

[15] Pal, S., Tak, Y.K., Song, J.M., 2007. Does the Antibacterial Activity of Silver Nanoparticles Depend on the Shape of the Nanoparticle? A Study of the Gram-Negative Bacterium *Escherichia coli*. Appl Environ Microbiol, 2007, 73, 1712–1720.

[16] Singh, P., Kim, Y.-J., Zhang, D., Yang, D.-C., 2016. Biological Synthesis of Nanoparticles from Plants and Microorganisms. Trends in Biotechnology, 2016, 34, 588–599.

[17] Crump, B.C., Hopkinson, C.S., Sogin, M.L., Hobbie, J.E., 2004. Microbial Biogeography along an Estuarine Salinity Gradient: Combined Influences of Bacterial Growth and Residence Time. Appl Environ Microbiol, 2004, 70, 1494–1505.

[18] Patra, J.K., Baek, K.-H., 2014. Green Nanobiotechnology: Factors Affecting Synthesis and Characterization Techniques. Journal of Nanomaterials, 2014, 2014, 417305.

[19] Gürtler, V., Stanisich, V.A., 1996. New approaches to typing and identification of bacteria using the 16S-23S rDNA spacer region. Microbiology, 1996, 142, 3–16.

[20] Tamura, K., Stecher, G., Kumar, S., 2021. MEGA11: Molecular Evolutionary Genetics Analysis Version 11. Molecular Biology and Evolution, 2021, 38, 3022–3027.

[21] Fu, L.-M., Hsu, J.-H., Shih, M.-K., Hsieh, C.-W., et al., 2021. Process Optimization of Silver Nanoparticle Synthesis and Its Application in Mercury Detection. Micromachines, 2021, 12, 1123.

[22] Paramelle, D., Sadovoy, A., Gorelik, S., Free, P., et al., 2014. A rapid method to estimate the concentration of citrate capped silver nanoparticles from UV-visible light spectra. Analyst, 2014, 139, 4855.

[23] Ashraf, J.M., Ansari, M.A., Khan, H.M., Alzohairy, M.A., Choi, I., 2016. Green synthesis of silver nanoparticles and characterization of their inhibitory effects on AGEs formation using biophysical techniques. Sci Rep, 2016, 6, 20414.

[24] Ben-Efraim, Y., Avnir, D., 2013. Organic Ag–Hg amalgam composite materials. Acta Materialia, 2013, 61, 7384–7391.

[25] Asif, M., Yasmin, R., Asif, R., Ambreen, A., et al., 2022. Green Synthesis of Silver Nanoparticles (AgNPs), Structural Characterization, and their Antibacterial Potential. Dose-Response, 2022, 20, 15593258221088709.

[26] Iwashita N., n.d. *Materials Science and Engineering of Carbon.*, Oxford, UK, pp. 7-25.

[27] Lowry, OliverH., Rosebrough, NiraJ., Farr, A.L., Randall, RoseJ., 1951. PROTEIN MEASUREMENT WITH THE FOLIN PHENOL REAGENT. Journal of Biological Chemistry, 1951, 193, 265–275.

[28] DuBois, Michel., Gilles, K.A., Hamilton, J.K., Rebers, P.A., Smith, Fred., 1956. Colorimetric Method for Determination of Sugars and Related Substances. Anal. Chem., 1956, 28, 350–356.

[29] Fagbayi, T., Ogbonnia, S., Ogbunugafor, H.A., Okochi, V.I., et al., 2008. Estimation of Cholesterol Level in Different Brands of Vegetable Oils. Pak. J. Nutr., 2008, 8, 57–62.

[30] Kassem, A., Abbas, L., Coutinho, O., Opara, S., et al., 2023. Applications of Fourier Transform-Infrared spectroscopy in

microbial cell biology and environmental microbiology: advances, challenges, and future perspectives. Front. Microbiol., 2023, 14, 1304081.

[31] Dhoondia, Z.H., Chakraborty, H., 2012. *Lactobacillus* Mediated Synthesis of Silver Oxide Nanoparticles. Nanomaterials and Nanotechnology, 2012, 2, 15.

[32] Syame, S.M., Mansour, A.S., Khalaf, D.D., Ibrahim, E.S., Gaber, E.S., 2020. Green Synthesis of Silver Nanoparticles Using Lactic Acid Bacteria: Assessment of Antimicrobial Activity. WVJ, 2020, 10, 625–633.

[33] Garmasheva, I., Kovalenko, N., Voychuk, S., Ostapchuk, A., et al., 2016. Lactobacillus species mediated synthesis of silver nanoparticles and their antibacterial activity against opportunistic pathogens in vitro. Bioimpacts, 2016, 6, 219–223.

[34] Huang, H., Shan, K., Liu, J., Tao, X., et al., 2020. Synthesis, optimization and characterization of silver nanoparticles using the catkin extract of Piper longum for bactericidal effect against food-borne pathogens via conventional and mathematical approaches. Bioorganic Chemistry, 2020, 103, 104230.

[35] Morones, J.R., Elechiguerra, J.L., Camacho, A., Holt, K., et al., 2005. The bactericidal effect of silver nanoparticles. Nanotechnology, 2005, 16, 2346–2353.

[36] Mustapha, T., Misni, N., Ithnin, N.R., Daskum, A.M., Unyah, N.Z., 2022. A Review on Plants and Microorganisms Mediated Synthesis of Silver Nanoparticles, Role of Plants Metabolites and Applications. IJERPH, 2022, 19, 674.